Synchronization Analysis of Autonomous Microwave Circuits Using New Global-Stability Analysis Tools

Almudena Suárez, *Member, IEEE,* José Morales, *Member, IEEE,* and Raymond Quéré, *Member, IEEE*

***Abstract*— A new spectral-balance technique for the global-stability analysis of autonomous circuits is presented in this paper. This technique relies on the introduction of measuring probes into the circuit and it allows a simple determination of both bifurcation diagrams and bifurcation loci as a function of any suitable parameter. Through the proposed algorithms, this kind of analysis can be easily added to any existing software, since it is performed externally to the harmonic-balance (HB) calculation. Due to its local nature, it also allows an easy selection of the bifurcation parameters, which spreads the simulation possibilities. Both periodic and quasi-periodic regime simulations are possible, and bifurcations are detected in both operating modes. The synchronization phenomenon in injected oscillators and frequency dividers is also analyzed in detail for an accurate prediction of the operating bands. The simulation techniques are illustrated by means of their application to a cubic nonlinearity oscillator. They are then used for the stability analysis of a monolithic microwave integrated circuit (MMIC) divider by two operating in the millimetric range. A very good agreement has been obtained with the experimental results.**

***Index Terms*—Bifurcation, continuation method, frequency divider, stability, synchronization.**

I. Introduction

THE HARMONIC-BALANCE (HB) method allows an efficient analysis of forced nonlinear regimes. However, in the case of autonomous or synchronized regimes, it must be complemented with special techniques in order to avoid its convergence toward trivial solutions [1], [2]. One of the most powerful is the measuring probes technique [2]. A probe is an independent source operating at the autonomous or synchronized fundamental with a filter, eliminating its influence at all the other frequencies. The probe must also satisfy a nonperturbation condition of the steady state, which is provided by a simple mathematical equation. By means of the probe, the circuit may be simulated as if it operated in a forced regime, which allows a straightforward application of the HB technique. In this paper, some modifications are introduced in this technique to make it more easily applicable to any existing HB software. In the new resolution method, it is taken into account that the HB independent variables are related to the probe value through the HB equations. Thus, with the aid of an existing HB approach, it is possible to consider an absolute dependence of the probe nonperturbation equation on the probe variables, such as amplitude, phase, or frequency. One of these variables can always be fixed in advance according to the regime to be simulated, so the resulting system will be of order two, which greatly reduces the complexity of the calculation.

When one or more parameters are considered, bifurcation phenomena such as synchronization, hysteresis, or frequency division must be accurately detected for a good prediction of the circuit behavior. The solution paths are constituted by the set of solutions of the HB equations that result from the variation of a parameter. Here, they are obtained by introducing the parameter into the probe equations and applying a continuation technique [3] to these equations instead of the HB system. This makes it possible to implement this analysis separately from the HB calculation. The method is applicable both for periodic and quasi-periodic solution paths. This allows a more accurate analysis of the transformations from one regime to another, which often show hysteresis phenomena. Although a probe formalism for bifurcations had been established before [2], this was based on the root calculation of the HB-system characteristic determinant [2], [4], using the probe for modeling the injection generator (substitution probe) [2]. Many technical aspects of the method change when measuring (nonperturbing) probes are used. Actually, considering the absolute dependence of the probe on its own variables, important bifurcation phenomena can be easily detected. These are mainly branching and turning points.

Branching: For a given parameter value, a solution branch starts or ends. This is characteristic of Hopf bifurcations and frequency division by two. When the branch is traced by means of a probe, its beginning and end correspond to a zero value of the probe amplitude. This allows a simple detection of the branching points.

Turning Point: The turning points at which the solution path shows an infinite or undetermined slope, indicating the creation or annihilation of solution states [4]. The curves corresponding to the probe variables (e.g., amplitude, phase, or operating frequency) also exhibit turning points for the same parameter values, as will be shown. The probe absolute system allows a simple detection of these points, due to its reduced 2×2 dimension.

Manuscript received November 8, 1996; revised February 13, 1998.

A. Suárez is with the Departmento de Ingenieria de Comunicaciones, Universidad de Cantabria, 39005 Santander, Spain.

J. Morales was with the Departmento de Ingenieria de Comunicaciones, Universidad de Cantabria, 39005 Santander, Spain. He is now with the Electronic Department, University of Tachira, 5001 Tachira, Venezuela.

R. Quéré is with IRCOM, URA CNRS 356 IUT de Brive, 19100 Brive, France.

Publisher Item Identifier S 0018-9480(98)03162-7.

0018–9480/98$10.00 © 1998 IEEE

Bifurcation loci (on a two-parameter plane) may thus be obtained by imposing simple conditions to the measuring probe introduced into the circuit. This avoids the more demanding root calculation of the HB characteristic determinant [2], [4].

In the engineering literature, the term *phase-locked* is often applied to any periodic state of an injected oscillator. However, from an autonomous quasi-periodic regime with two nonrationally related fundamentals, there are two different phenomena leading to a periodic behavior as a parameter is modified: the synchronization, when the two fundamentals become rationally related, and the inverse Hopf bifurcation, or asynchronous extinction of the autonomous frequency. The former only takes place for a relatively narrow band, around the free-running oscillation frequency, or one of its harmonic components, and it is associated to turning points of periodic bifurcation diagrams. From a geometrical viewpoint, at the turning points (also called saddle-node bifurcations) of a stable periodic regime, a stable node and a saddle of the Poincare mapping collide in a single equilibrium point (saddle node) and disappear for further parameter variation [5], [6]. Generally speaking, the system solution should then jump to another stable solution, but if no one is encountered, stable and unstable manifolds will give rise to a limit cycle of the mapping [5], [6], i.e., to a quasi-periodic regime. This may be understood as a loss of synchronization of the initial periodic regime. Turning points may thus correspond either to jump or phase-locking phenomena. Here, some hints are provided in order to distinguish both types of turning points from the bifurcation loci. The transformation of the quasi-periodic paths into a synchronized periodic response is also studied in detail.

For an easy understanding of the proposed techniques, these are going to be applied first to a cubic nonlinearity oscillator. Then, a monolithic microwave integrated circuit (MMIC) frequency divider by two in the millimetric range will be analyzed. They will be used as examples in the analysis of the synchronization phenomena and their behavior will be compared from a bifurcation point of view.

II. Steady-State Analysis

In the HB formulation, the overall circuit (see Fig. 1) is split into an embedding linear circuit, independent generators $\mathbf{g}(t)$, and nonlinear sources $\mathbf{y}(t)$ controlled by the independent variables $\mathbf{x}(t)$. The HB system is then obtained by equating all the spectral components of the Fourier transforms of $\mathbf{g}(t)$, $\mathbf{x}(t)$, and $\mathbf{y}(t)$, and can be written as [7]

$$\mathbf{H}_b(\mathbf{X}) = [A_{\mathbf{X}}]\mathbf{X} - [A_{\mathbf{Y}}]\mathbf{Y}(\mathbf{X}) - [A_{\mathbf{G}}]\mathbf{G} = 0 \qquad (1)$$

where $\mathbf{X}$, $\mathbf{Y}$, and $\mathbf{G}$ are vectors, respectively, containing the spectral components of $\mathbf{x}(t)$, $\mathbf{y}(t)$, and $\mathbf{g}(t)$. The matrices are obtained from the analysis of the linear part of the circuit. The frequency components will be given by ω_k with $-N_C \leq k \leq N_C$.

The application of HB is straightforward in the case of forced regimes, but in case of autonomous or synchronized operation there might be some problems of convergence toward trivial solutions. When a measuring probe [2] at the autonomous or synchronized frequency is introduced into the circuit, as shown in Fig. 2, the analysis may be performed as in the forced regime, taking advantage of the efficiency of HB in forced operation. For the resulting solution to be valid, the probe must satisfy a nonperturbation condition of the steady state [2]. According to the type of probe (voltage or current source), this condition will be given by

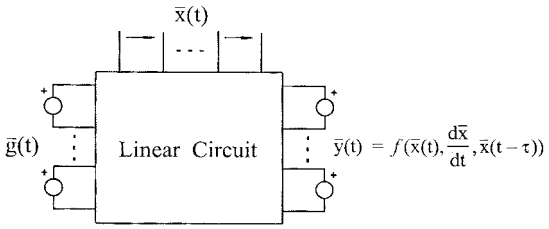

Fig. 1. HB partitioning.

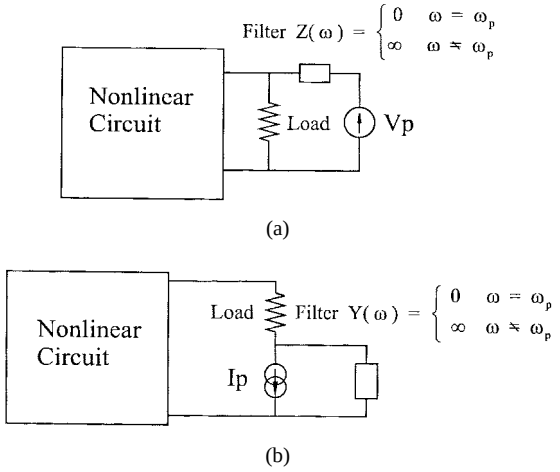

Fig. 2. Probes configuration. (a) Voltage probe. (b) Current probe.

$$S = \frac{I_p}{V_p} = 0 \quad \text{for a voltage probe}$$
$$S = \frac{V_p}{I_p} = 0 \quad \text{for a current probe} \qquad (2)$$

where V_p and I_p are, respectively, the probe voltage and current.

The probe is characterized by its amplitude A_p, operating frequency ω_p, and phase Φ_p. However, depending on the type of regime to be analyzed, one of them can always be fixed in advance [2]. Hereafter, the two probe variables to be determined will be called p_1 and p_2. These variables will be A_p and ω_p for autonomous regimes and A_p and Φ_p for synchronized regimes [2]. The total system will then be

$$\mathbf{H}_b(\mathbf{X}, p_1, p_2) = 0 \qquad (3a)$$
$$\mathbf{S}(\mathbf{X}, p_1, p_2) = 0 \qquad (3b)$$

where $\mathbf{H}_b$ are the spectral-balance equations and $\mathbf{S}$ is the vector composed of the real and imaginary parts of the ratio (2).

The system (3) can be solved considering a partial dependence of the probe and HB equations on the nonlinearity controlling variables $\mathbf{X}$ and the probe variables p_1 and p_2 [2]. However, including the probe in the generator vector $\mathbf{G}$, the

vector $\mathbf{X}$ corresponding to every $\mathbf{p}$ value, with $\mathbf{p} = (p_1, p_2)$ can be obtained through the HB approach, as stated in (1). An absolute dependence of the probe equations on the probe vector $\mathbf{p}$ may then be considered as follows:

$$\mathbf{S}[\mathbf{X}(p_1, p_2), p_1, p_2] \equiv \mathbf{S}(p_1, p_2) = 0. \tag{4}$$

The solving strategy adopted here is thus based on a two-tier process where the pure HB equation constitutes the inner loop. In this way, a system of only two unknowns in two equations is obtained. Although more demanding in terms of computer time, this method has the advantage of being easily applicable to existing software since it can be implemented separately from the HB calculation.

III. Global-Stability Analysis

A. Probe-Continuation Method

For obtaining the evolution of the circuit steady solution when one of its parameters is continuously modified, this parameter should be introduced into the probe equations

$$\begin{aligned} \mathbf{S}_r(p_1, p_2, \mu) &= 0 \\ \mathbf{S}_i(p_1, p_2, \mu) &= 0 \end{aligned} \tag{5}$$

where the subindexes indicate real and imaginary parts. This is a system of three unknowns in two equations that provides the solution path. In general, this curve will be multivalued and this is why a continuation method must be used. The Jacobian matrix of the probe equations is introduced first:

$$[J_{\mathbf{S}}] = \begin{bmatrix} \dfrac{\partial \mathbf{S}_r}{\partial p_1} & \dfrac{\partial \mathbf{S}_r}{\partial p_2} \\ \dfrac{\partial \mathbf{S}_i}{\partial p_1} & \dfrac{\partial \mathbf{S}_i}{\partial p_2} \end{bmatrix}. \tag{6}$$

Once a solution $\mathbf{X}^n(\mathbf{p}^n)$ has been determined for the parameter value μ^n, the prediction for the next point of the path $\mathbf{X}_p^{n+1}(\mathbf{p}_p^{n+1})$ corresponding to $\mu^n + \Delta\mu$ may be obtained by linearizing the probe equations about $\mathbf{p}^n$ as follows:

$$[J_{\mathbf{S}}]^n(\mathbf{p}_p^{n+1} - \mathbf{p}^n) + \left[\frac{\partial \mathbf{S}}{\partial \mu}\right]^n \Delta\mu = 0. \tag{7}$$

After a possible parameters exchange, the correction of the predicted value is performed by means of the Newton–Raphson algorithm. From (7), the infinite slope or turning points of the solution curve as a function of the continuation parameter μ will satisfy

$$\begin{bmatrix} \dfrac{\Delta p_1}{\Delta \mu} \\ \dfrac{\Delta p_2}{\Delta \mu} \end{bmatrix} = [J_{\mathbf{S}}]^{-1} \cdot \left[\frac{\partial \mathbf{S}}{\partial \mu}\right] = \infty. \tag{8}$$

Thus, they will correspond to a zero value of the determinant of the Jacobian matrix, as given by (6).

This continuation method is easily implementable on the computer since no modifications of the HB formulation are needed. Actually, the selection of a new parameter only involves modifications in the few subroutines dealing with the derivatives calculation of the function $\mathbf{S}$. This method is especially suitable for obtaining the solution paths in autonomous operating modes such as those corresponding to tuned oscillators or to the autonomous quasi-periodic solutions of injected oscillators. Actually, for obtaining these paths from a traditional continuation approach applied to the HB system (aside from the HB Jacobian matrix), two sets of derivatives of the HB functions will be needed: with respect to the parameter μ and the autonomous frequency ω_a, which varies along the path. By applying (7), no derivatives of the HB functions with respect to μ or ω_a are calculated.

B. Stability Analysis

For determining the stability of a given solution point $\mathbf{X}_0(\mu)$, a perturbation of the form $e^{(\sigma + j\omega)t}$ will be considered [4]. Due to its small value, the new solution point may be expressed as $\mathbf{X} = \mathbf{X}_0 + \Delta\mathbf{X}$ with the perturbation vector $\Delta\mathbf{X}$ having frequency components given by $\omega_k + \omega - j\sigma$. This perturbation vector must also satisfy the HB equations, and since there are no generators at the perturbation frequencies, an homogeneous system (also called *characteristic system*) will result. For solutions $\Delta\mathbf{X}$ different from zero to exist, the system determinant must be equal to zero. The steady solution $\mathbf{X}_0$ will be stable when all the determinant roots have $\sigma < 0$ and bifurcations (or qualitative stability changes) will be obtained for the parameter values satisfying [4]

$$\begin{aligned} \det[\Gamma(\mu, \mathbf{X}_0, \omega)] &= 0 \\ \frac{d\sigma}{d\mu} &\neq 0 \end{aligned} \tag{9}$$

where Γ is the characteristic matrix.

Equation (9) provides the general condition for local type bifurcations, i.e., involving a single point [5]. The vector $\mathbf{X}_0$ is the steady-state solution with any number of fundamentals corresponding to the parameter value μ. Different sorts of bifurcations are possible depending on the initial regime and the frequency value ω satisfying (9). The new method is based on the properties of the probe amplitude or associated determinant at the bifurcation points. In the Appendix, a discussion is presented about the equivalence between the bifurcation conditions obtained from the new method and the general equation (9). Three different regimes will be considered: autonomous periodic, periodic with external excitation, and autonomous quasi-periodic.

A. Autonomous Periodic

1) Primary Hopf Bifurcation: Start of a Free-Running Oscillation: When applying (9) to a dc regime of a potentially autonomous circuit, the corresponding solutions provide the primary Hopf bifurcation points, at which RF solutions with ω as fundamental frequency appear or disappear.

When introducing a probe into the circuit, the primary Hopf bifurcation points are given by the solutions of the probe absolute system for a zero value of the probe amplitude, as this is the limit condition for the existence of an autonomous solution. Actually, in an autonomous solution path, a probe value may be assigned to each steady oscillation, while as soon as this autonomous solution is extinguished, the nonperturbation

condition (4) cannot be satisfied for any probe amplitude or frequency. Due to the continuity of the probe equations, the probe amplitude will tend to a zero value as the inverse Hopf bifurcation point is approached.

The practical resolution for primary Hopf bifurcation points may be carried out by imposing the probe a threshold amplitude value ϵ. The equation system to be solved will be

$$\begin{aligned} \mathbf{S}_r(\omega_p, \overline{\mu}) &= 0 \\ \mathbf{S}_i(\omega_p, \overline{\mu}) &= 0 \\ A_p &= \epsilon \end{aligned} \tag{10}$$

where the probe frequency ω_p is of course equal to the unknown autonomous frequency ω_a. The vector μ may be composed of one or two parameters. In case of two elements (μ_1, μ_2), a bifurcation locus will be obtained on the plane (μ_1, μ_2). Possible parameters are bias voltages or tuning elements. The application of a Nyquist analysis [4] provides a good initial estimate of ω_a for a given parameter value and (10) is easily solved through the Newton–Raphson method. This must be complemented with a continuation technique when a locus is to be obtained.

2) Turning Points: When tracing an oscillator solution path as a function of a tuning parameter, turning points giving rise to jump or hysteresis phenomena are often encountered. According to (8), these points will satisfy

$$\det[J_{\mathbf{S}}] = \frac{\partial \mathbf{S}_r}{\partial A}\frac{\partial \mathbf{S}_i}{\partial \omega_a} - \frac{\partial \mathbf{S}_i}{\partial A}\frac{\partial \mathbf{S}_r}{\partial \omega_a} = 0. \tag{11}$$

Due to the absolute dependence of the $\mathbf{S}$-function on the probe variables, the above determinant agrees with the Kurokawa stability function [8] for free-running oscillators. Here, the multiharmonic nature of the circuit solution is taken into account in the derivatives calculation (through HB). The turning points can thus be calculated by applying

$$\begin{aligned} \mathbf{S}_r(A_p, \omega_p, \overline{\mu}) &= 0 \\ \mathbf{S}_i(A_p, \omega_p, \overline{\mu}) &= 0 \\ \det[J_{\mathbf{S}}(A_p, \omega_p, \overline{\mu}] &= 0 \end{aligned}$$

where $\omega_p = \omega_a$. Either a single bifurcation point or a locus may be obtained according to the dimension of μ.

B. Periodic Regime With External Excitation

From a periodic regime of fundamental ω_{in} provided by the external generator, different sorts of bifurcations are possible.

1) Indirect or I-Type Bifurcation: Frequency Division by Two: I-type bifurcations are solutions of (9) for $\omega = \omega_{\text{in}}/2$. At these points, a divided-by-two solution appears or disappears [9]. By means of a probe, such solutions are obtained by fixing the probe frequency ω_p to $\omega_{\text{in}}/2$ and solving (4) for its phase and amplitude. At the I-type bifurcation points, the probe amplitude takes a zero value, which can be explained in a similar fashion to the autonomous case. The practical resolution is carried out from the following system:

$$\begin{aligned} \mathbf{S}_r(\phi_p, \overline{\mu}) &= 0 \\ \mathbf{S}_i(\phi_p, \overline{\mu}) &= 0 \\ A_p &= \epsilon \\ \omega_p &= \frac{\omega_{\text{in}}}{2}. \end{aligned} \tag{13}$$

For two elements in the vector μ, the I-type bifurcation locus is obtained.

2) Secondary Hopf Bifurcation: Appearance of an Autonomous Frequency: The secondary Hopf bifurcations are solutions of (9) for $\omega = \alpha\omega_{\text{in}}$ with $\alpha \in R$ and nonrational. At these points, a quasi-periodic solution of fundamentals ω_{in} and ω_a [9] will appear or disappear as the parameter is modified. The latter case will correspond to an inverse Hopf bifurcation. By means of a probe, the Hopf bifurcation points may be obtained by setting the probe amplitude to a threshold value ϵ and solving for the parameter value and the autonomous frequency ω_a

$$\begin{aligned} \mathbf{S}_r(\omega_p, \overline{\mu}) &= 0 \\ \mathbf{S}_i(\omega_p, \overline{\mu}) &= 0 \\ A_p &= \epsilon \end{aligned} \tag{14}$$

where the probe frequency ω_p is equal to ω_a. Due to the threshold amplitude value of the autonomous fundamental, the number of spectral components for the resolution of (14) may be greatly reduced.

3) Turning Points: At turning points, the path stability changes without any variation in the system fundamentals. Thus, they are solutions of (9) for $\omega = 0$. Using the probe method, the probe phase and amplitude will be the variables to be solved. Taking (8) into account, turning points may be calculated by applying

$$\begin{aligned} \mathbf{S}_r(A_p, \phi_p, \overline{\mu}) &= 0 \\ \mathbf{S}_i(A_p, \phi_p, \overline{\mu}) &= 0 \\ \mathrm{Det}[J_{\mathbf{S}}(A_p, \phi_p, \overline{\mu})] &= 0. \end{aligned} \tag{15}$$

Either a single bifurcation point or locus may be obtained according to the dimension of μ.

Turning points are associated to jump and hysteresis phenomena. However, as already discussed, they may also determine the end of phase-locked behavior. When tracing the loci of an injected oscillator on the traditional plane, given by the *input power* and the *input frequency*, the free-running oscillation point will always belong to one of the possible turning point loci (as it is a degenerated point, obtained for zero input power). The synchronization phenomenon will be treated in greater detail in Section III-B.3 and the application section.

C. Autonomous Quasi-Periodic Regime

An initial autonomous quasi-periodic regime will now be considered. The two fundamentals will be ω_{in} and the circuit autonomous frequency ω_a. Possible bifurcations from this

regime will be turning points and the appearance or disappearance of a second autonomous fundamental. In addition to that, the vanishing of autonomous quasi-periodic paths may be due to two different phenomena: synchronization of the two fundamental frequencies and extinction of the autonomous frequency ω_a by an inverse Hopf bifurcation. Each of these phenomena will be treated in the following subsections.

1) Synchronization: Starting from an autonomous quasi-periodic regime, as the parameter is modified, the autonomous frequency is modified too. Synchronization takes place when the two fundamentals ω_{in} and ω_a become commensurable for a certain parameter range. In order to detect the approaching of a synchronization parameter value, the rotation number r is going to be introduced [6]. This number is defined as the ratio between the two independent fundamentals

$$r(\overline{\mu}) = \frac{\omega_a(\overline{\mu})}{\omega_{\mathrm{in}}}.$$

At the synchronization points, r becomes rational, remaining constant for a certain parameter set.

The transformation suffered by the quasi-periodic paths at the synchronization points depends on the value that the rotation number r reaches at these points.

i) $r = 1$: The autonomous component vanishes and the external one becomes the fundamental of the new periodic regime. This is the case of an injected oscillator. At the synchronization points, the probe amplitude A_p takes a zero value.

ii) $r = m/n \neq 1$ (with m and n integers): The probe value approaches that of the $m \cdot (\omega_{\mathrm{in}}/n)$ frequency component in the new periodic regime. For $r = 1/n$, the autonomous component from the quasi-periodic regime becomes the system fundamental.

The rational ratio between the fundamental frequencies at the synchronization points leads to a degeneration of the quasi-periodic HB system, making it very difficult to detect these points from a quasi-periodic point of view. In periodic regime, the synchronization of fundamentals is given by a turning point of the solution path [5], [6] (which is not true for the inverse Hopf bifurcations). The synchronization points may thus be obtained from the same condition (15). However, it will be necessary to distinguish these synchronization points from the periodic path turning points associated to hysteresis and jumps. A technique will be provided in the application section.

2) Hysteresis: The quasi-periodic paths can also show turning points, responsible for hysteresis or jump phenomena. From the probe point of view, they will correspond to zero values of its associated determinant [see (8)]. The quasi-periodic turning points are thus obtained from the system

$$\begin{aligned} \mathbf{S}_r(A_p, \omega_p, \overline{\mu}) &= 0 \\ \mathbf{S}_i(A_p, \omega_p, \overline{\mu}) &= 0 \\ \det[\mathbf{S}(A_p, \omega_p, \overline{\mu}] &= 0 \end{aligned} \tag{17}$$

with $\omega_p = \omega_a$. The determination of the turning points in the quasi-periodic paths is extremely important for a good characterization of the circuit behavior. Actually, when the quasi-periodic path vanishing is due to an inverse Hopf bifurcation, a turning point often occurs for parameter values beyond the Hopf bifurcation [10], [11] and is thus responsible for the transformation from autonomous quasi-periodic to periodic regime through a jump phenomenon. As has been shown in [12], coexistence of synchronized/divided and quasi-periodic paths is even possible in these cases.

3) Hopf Bifurcation: Appearance of a Second Autonomous Fundamental: The appearance of a second autonomous fundamental may be detected through harmonic balance by introducing a second probe into the circuit. The system to be solved will then be

$$\begin{aligned} \mathbf{S}(A_p^1, \omega_p^1, \omega_p^2, \overline{\mu}) &= 0 \\ \mathbf{S}(A_p^1, \omega_p^1, \omega_p^2, \overline{\mu}) &= 0 \\ A_p^2 &= \epsilon \end{aligned} \tag{18}$$

where A_p^2 and ω_p^2 are the second probe amplitude and frequency.

As a final comparison between the traditional approach for the bifurcation point calculation, based on (9) and the new probe method, it may be said that the former is less computer time consuming, but more demanding from a programming point of view. In addition to that, it is often less accurate when applied for obtaining the bifurcation loci. This is due to the difficulties in choosing, when two parameters vary, a proper threshold value for the zeros of the characteristic determinant in the numerical resolution. In order to clarify this point, the simulation of two periodic paths showing turning points has been carried out [see Fig. 3(a)]. According to Section III-B.2, the HB characteristic determinant as well as the probe determinant should take a zero value at these points. The variations of the HB determinant along two paths, corresponding to 0 and 6 dBm input power, respectively, are shown in Fig. 3(c) and (d). As can be seen, the bifurcation prediction is accurate. However, the resolution of (9) for the two parameters *input power, input frequency* (in order to obtain the turning point locus) would be very difficult due to the big change in the determinant magnitude as the input power is modified (from order 10^{13} to 10^{10} in this example). The same big variations have been found for other two-parameter analysis. As can be seen in Fig. 3(b), the variation range of the probe determinant is similar in both cases. The accuracy problems of the HB determinant are even more serious in quasi-periodic regime, due to the high dimension of the characteristic matrix. In the probe method, the system to be analyzed is always a 2×2 system, whatever the number of frequency components taken into account, which greatly reduces the resolution difficulties. For the branching point bifurcations, the threshold value to be imposed always corresponds to a voltage or current variable, which makes the threshold assignation much simpler than for the determinant of a high-order matrix.

IV. Applications

A. Cubic Nonlinearity Oscillator

The stability analysis method proposed here has been applied to the cubic nonlinearity oscillator of Fig. 4. This circuit

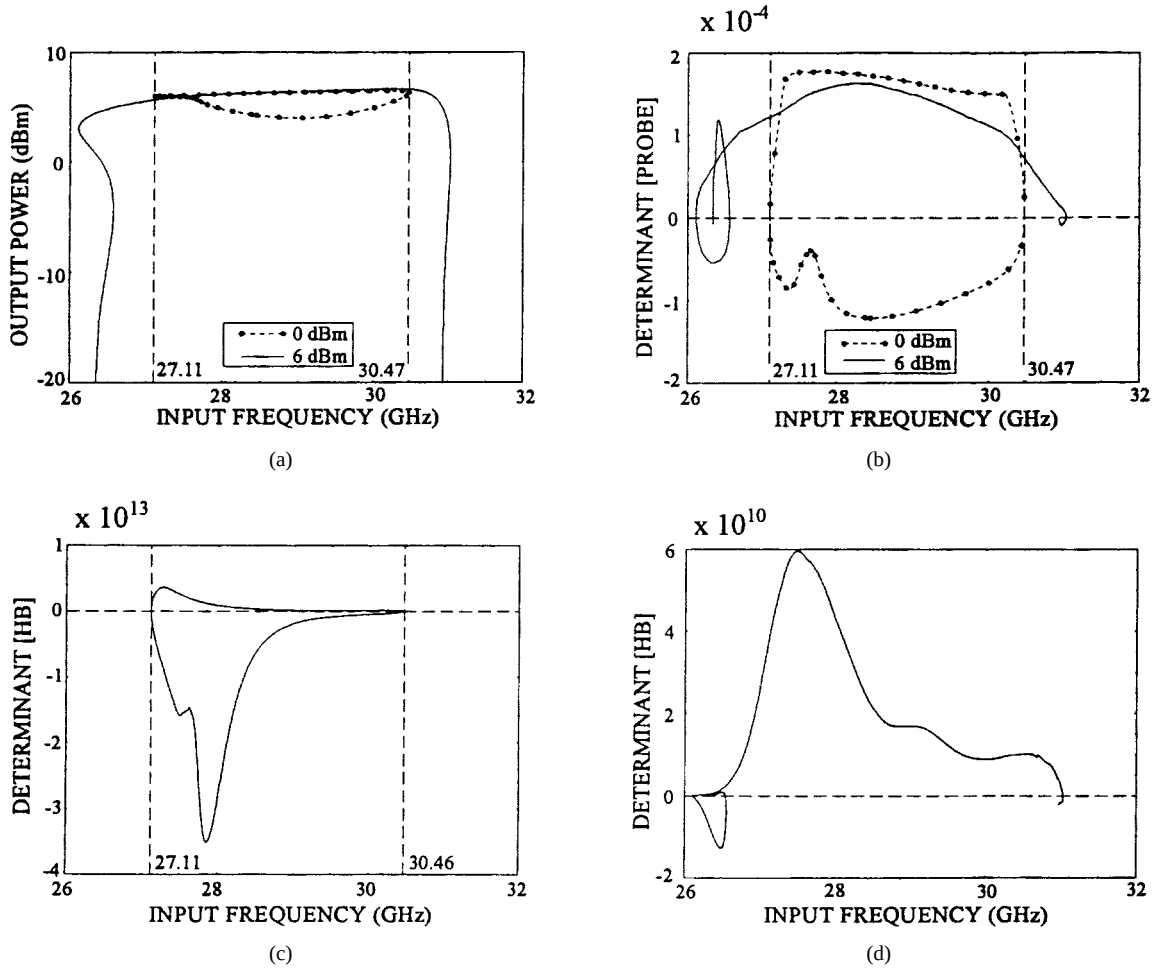

Fig. 3. Turning point detection in MMIC frequency divider. (a) Constant input power paths. (b) Probe determinant. (c)–(d) HB characteristic determinant.

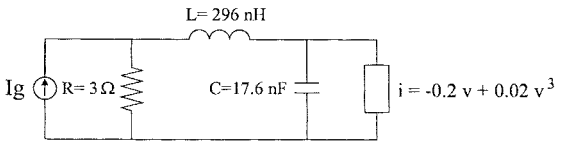

Fig. 4. Cubic nonlinearity oscillator.

may exhibit two main modes of operation: phase-locked oscillator and self-oscillating mixer. Its bifurcation loci on the usual parameter plane, given by the input generator amplitude and frequency, are shown in Fig. 5. As already indicated, the free-running oscillation always belongs to one of the possible turning point loci in the periodic regime. In Fig. 5, this point is given by O and the corresponding locus by $AOCD$. This turning-point locus may contain both synchronization and jump points. Its two common points with the Hopf bifurcation locus (at which the latter originates) are solutions of (15) for a zero value of the probe amplitude and, in this example, are given by A and D. These points will provide a good estimate for the border between synchronization and jump behavior. Actually, for $I_g < I_a$ and $I_g < I_D$ the turning-point curve must correspond to synchronization, as the Hopf locus is never traversed. For more accuracy, the possible existence of "saddle connections" [5] near the intersection points should be considered. Unlike other bifurcations commonly treated in

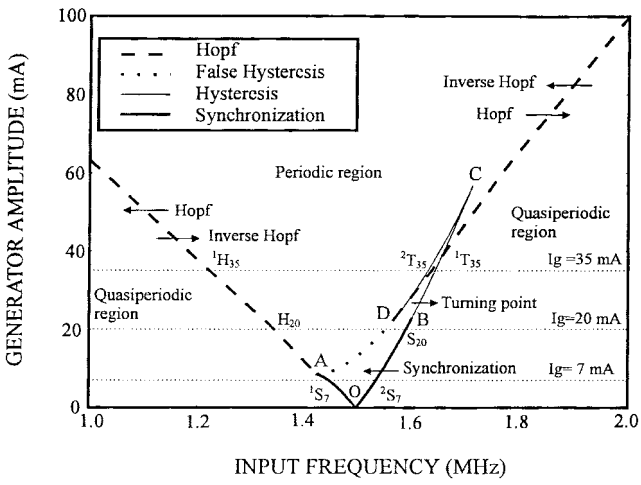

Fig. 5. Bifurcation loci for the cubic nonlinearity oscillator.

the microwave literature, these are bifurcations of global type, involving a special global configuration of invariant manifolds [5]. Although its study is beyond the scope of this paper, some preliminary detections have been carried out by analyzing the coalescence of the quasi-periodic solutions and the unstable (saddle) periodic paths. To our calculation accuracy, the saddle connection curve remains close to the constant line $I_g = I_D$.

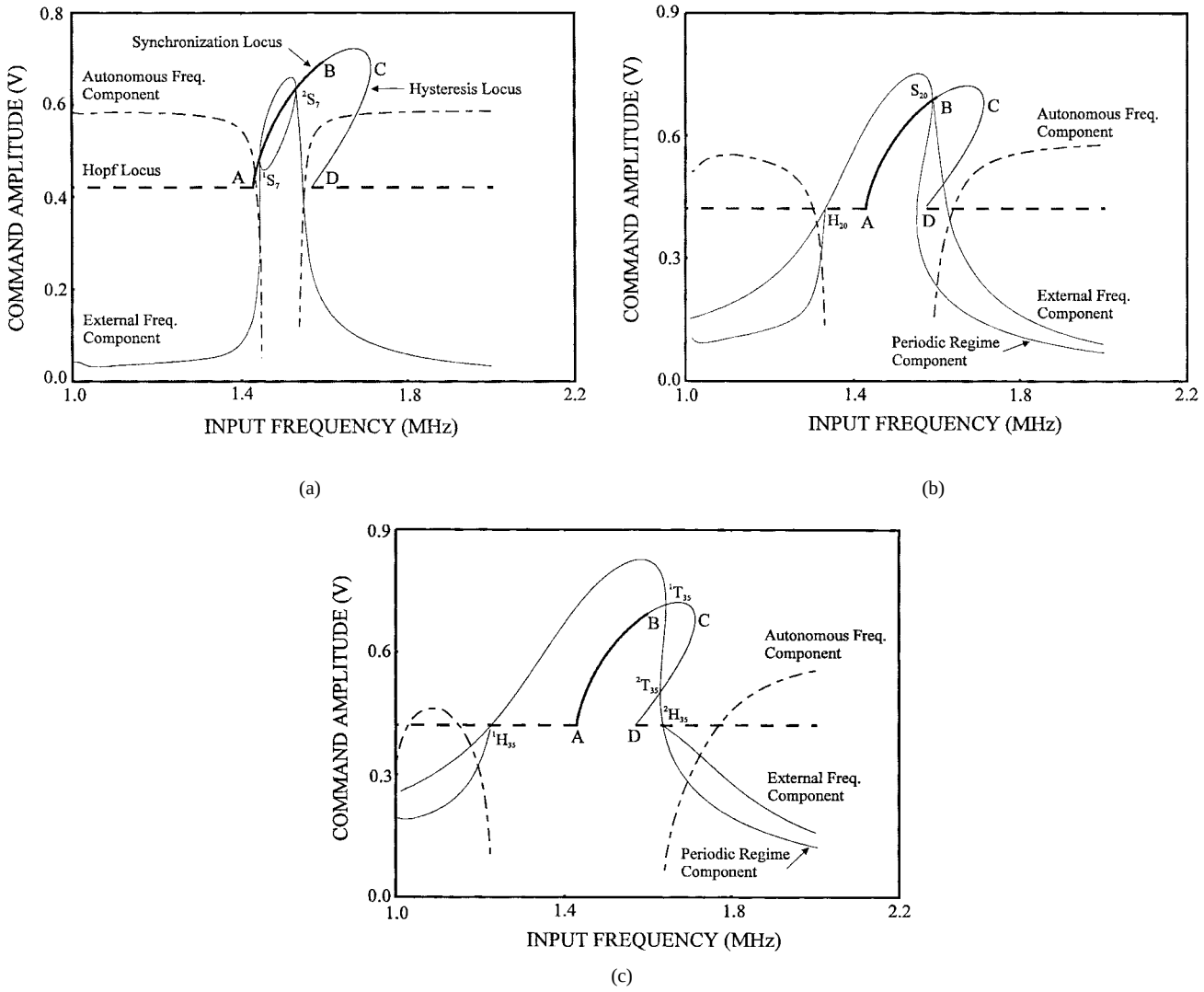

Fig. 6. Bifurcation diagrams as a function of input frequency for the cubic nonlinearity oscillator. (a) For input generator amplitude $I_g = 7$ mA. (b) For $I_g = 20$ mA. (c) For $I_g = 35$mA.

In Fig. 6, several bifurcation diagrams as a function of input frequency for different input current amplitudes, have been traced, including both periodic and quasi-periodic paths. Since in quasi-periodic regime there are two fundamental frequencies, a solution path is traced for each of them. The synchronization, hysteresis, and Hopf loci have been superimposed. Periodic paths will be unstable inside turning point locus and below the Hopf locus. For $I_g = 7$ mA [see Fig. 6(a)], the periodic path intersects at both ends ($^1S_7$ and $^2S_7$) of the synchronization locus. Then the start of the quasi-periodic regime will be due on both sides to a loss of synchronization. For $I_g = 20$ mA [see Fig. 6(b)], the appearance of the quasi-periodic regime at the left side is due to a Hopf bifurcation (H_{20}). On the right side, there is a loss of synchronization (S_{20}) from which the periodic path becomes unstable. For $I_g = 35$ mA [see Fig. 6(c)], the appearance, on the left side of the quasi-periodic response is due a Hopf bifurcation ($^1H_{35}$). The right part cuts twice the hysteresis locus ($^1T_{35}$ and $^2T_{35}$), which will give rise to an actual hysteresis phenomenon. Then, the Hopf locus is traversed ($^2H_{35}$), with appearance of the quasi-periodic paths.

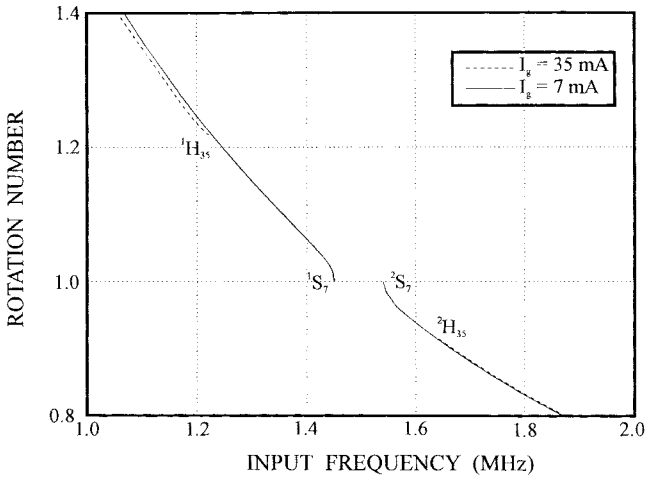

Fig. 7. Rotation number versus input frequency for input generator amplitudes $I_g = 7$ mA and $I_g = 35$ mA.

The evolution of the rotation number r as a function of input frequency for $I_g = 7$ mA and $I_g = 35$ mA is shown

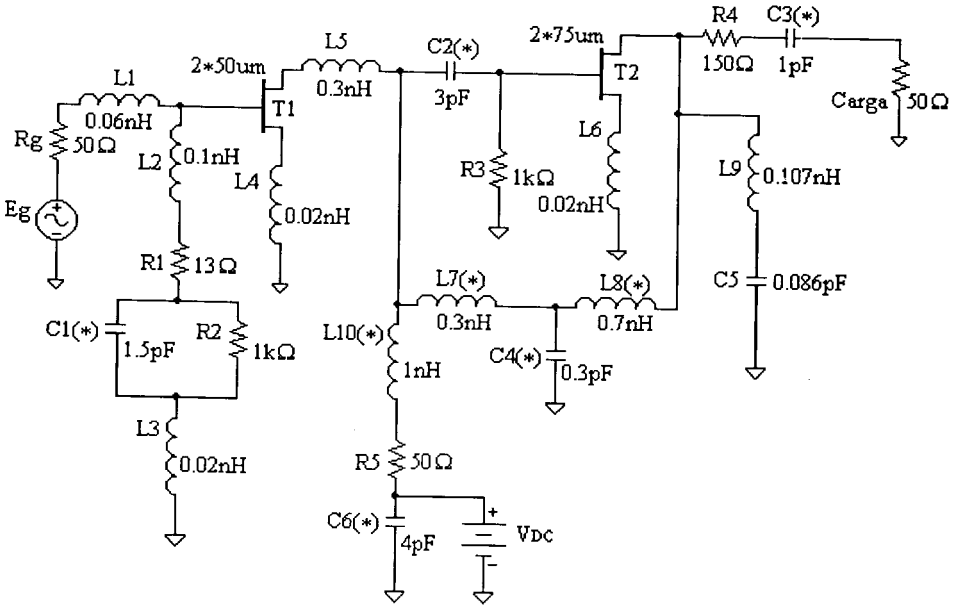

Fig. 8. Schematic of the MMIC frequency divider by two with input frequency 28 GHz.

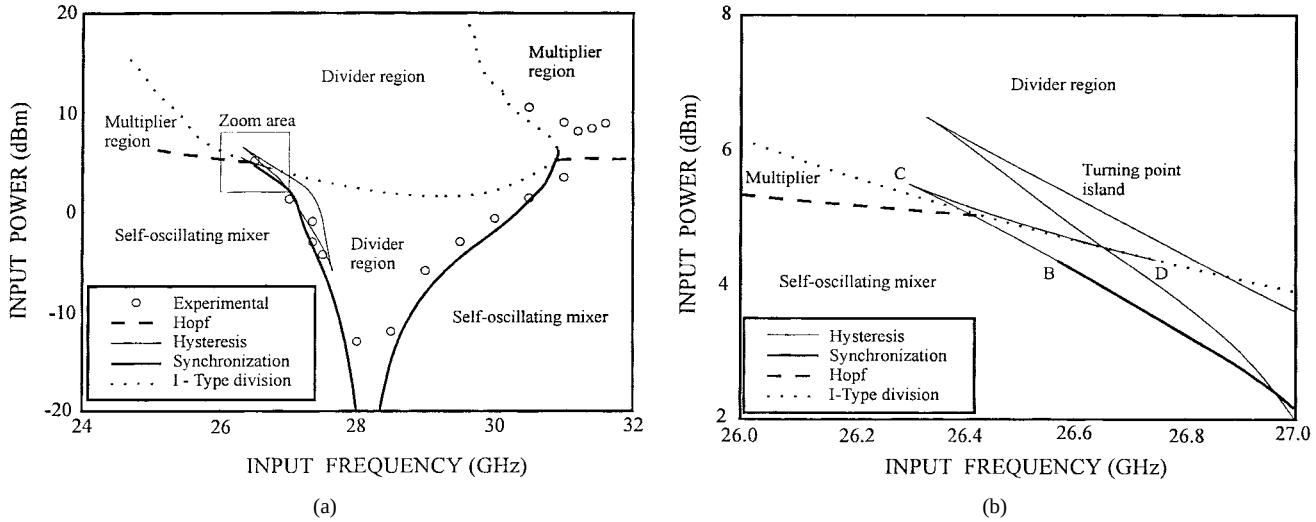

Fig. 9. Bifurcation loci of the MMIC frequency divider by two. (a) General view. (b) Expanded view.

in Fig. 7. For $I_g = 7$ mA, the rotation number reaches the unity value at the start points of periodic operation, which is characteristic of the synchronization phenomenon. For $I_g = 35$ mA, the transformation into periodic regime is due (at each end) to an inverse Hopf bifurcation. The value of the number r is nonrational at these points and far from unity.

B. MMMIC Frequency Divider in Millimetric Band

The schematic of a MMIC frequency divider by two [13] with central input frequency 28 GHz is shown in Fig. 8. A broad-band configuration [13] with two transistor stages has been used for the design. For a self-bias voltage of 3.5 V, the resulting bifurcation loci as a function of input power and frequency are shown in Fig. 9(a). Three main operation modes are to be noted: multiplier, self-oscillating mixer, and frequency divider. The frequency division may be due to two different phenomena: I-type bifurcation from a periodic regime, and second harmonic synchronization from a quasi-periodic one (below the Hopf locus).

As in this example, there may, in general, be one or more turning-point curves in periodic regime, located above or below the Hopf and I-type locus. The synchronization phenomenon will be associated to the turning-point curve containing the free-running oscillation (main turning-point locus). In Fig. 9(a), the small island on the left is a closed turning-point curve associated to jump and hysteresis phenomena in the divided paths. From this representation, it is not possible to predict the system state (synchronized or not) when the turning-point island is traversed, but this will be solved later. In Fig. 9(b), there is a zoom of the left side of the loci in which the common point D between the main turning-point locus and the Hopf locus may be observed. The locus provided by BCD is an hysteresis locus.

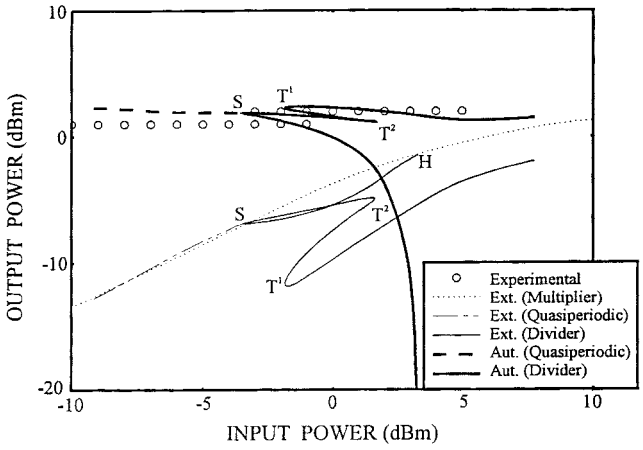

Fig. 10. Frequency-divider bifurcation diagram as a function of input power for input frequency $F_{\text{in}} = 27.35$ GHz.

In Fig. 10, the bifurcation diagram as a function of input power for constant input frequency 27.35 GHz has been traced. Synchronization takes place at point S. Below this point, the periodic paths (divider and multiplier) correspond to unstable solutions that will not be physically observable. The hysteresis phenomenon between T_1 and T_2 is due to the turning-point island and will be observable since it takes place in the stable synchronized section (above S). By tracing the quasi-periodic paths, it has been possible to distinguish the synchronization point from the other two turning points in the periodic path. This may be difficult when only periodic simulations are available. Here, we propose to trace the loci also on the planes defined by each parameter and a meaningful circuit variable, such as its output power. By superimposing the bifurcation diagram to be analyzed, the uncertainty about the order of occurrence of the different phenomena will be eliminated. Here, a loci representation has been carried out on the plane P_{in}–P_{out}, with P_{out} being the output power at the divided frequency. This has been split into two parts: one including the loci points for $\omega_{\text{in}}/2 \leq \omega_0$, with ω_0 being the free-running oscillation frequency, and the other including the loci points for $\omega_{\text{in}}/2 \geq \omega_0$. The former loci are shown in Fig. 11. For the Hopf and I-type loci, the output power at the divided frequency is equal to zero, so they both lie on the horizontal axis. The region inside the main turning-point locus is an unstable one. The intersection between the periodic solution path and the turning-point island takes place in the stable synchronized section, thus these intersection points will bring along an observable hysteresis phenomenon. Since there are no intersection points between the turning-point loci, this behavior pattern will be followed by all the bifurcation diagrams intersecting the island. Thus, it is possible to assure the physical existence of the island jump points.

V. Conclusions

Some modifications of the probe method for the analysis of autonomous and synchronized devices are presented here, allowing an easier application of this technique to any existing HB software. From the modified probe equations, a new continuation technique has been derived for tracing both periodic and quasi-periodic paths. A simple mathematical condition has also been obtained for each of the most important bifurcation types. The new technique, easily implementable on the computer, allows an accurate determination of the bifurcation loci, both from periodic and quasi-periodic regimes. The new method has been validated by comparing the results from these bifurcation loci with bifurcation diagrams obtained through the traditional approach. The synchronization phenomenon is also analyzed in detail.

All of the above techniques have been successfully applied to a cubic nonlinearity oscillator and a MMIC frequency divider with 28-GHz input frequency. The divider has been experimentally characterized, obtaining an excellent agreement with the simulation results.

Appendix

In this appendix, it will be shown how the general bifurcation (9) may be derived from the probe bifurcation conditions which validates the proposed technique. Since the condition for *turning point* has already been discussed in this paper, only the Hopf bifurcations (both from dc and periodic regimes) and the I-type bifurcation will be considered.

A. Hopf-Type Bifurcations

Let us suppose that for a parameter value μ the probe nonperturbation condition is satisfied for an incremental probe amplitude $A_p = \varepsilon$ and autonomous frequency $\omega_p = \omega_a$ as follows:

$$\mathbf{S}(\overline{\mu}, \omega_a) = 0 \quad \text{with } A_p = \epsilon. \tag{A.1}$$

Due to the probe equations continuity, the parameter μ must belong to a neighborhood of the parameter value μ_H, which is solution of (A.1) for $A_p = 0$. Through the HB equations, the $\mathbf{X}$ vector corresponding to the probe value (ϵ, ω_a) will be

$$\mathbf{X} = \mathbf{X}(\epsilon, \omega_a). \tag{A.2}$$

And in the time domain

$$\mathbf{x} = \mathbf{x}[p(t)] \tag{A.3}$$

with $p(t) = \epsilon \cdot \cos(\omega_a t)$. Since the probe value $p(t)$ is small, it will be possible to carry out a Taylor expansion of $\mathbf{x}(t)$ about $p = 0$. Then

$$\mathbf{x} \approx \mathbf{x}_0 + \left.\frac{\partial \mathbf{x}}{\partial p}\right|_0 \cdot p(t) \equiv \mathbf{x}(t)_0 + \Delta\mathbf{x}. \tag{A.4}$$

The vector $\mathbf{x}_0$ is the circuit solution for $p = 0$, which will be either constant or periodic. The derivatives $\partial \mathbf{x}_0/\partial p$ in the incremental term $\Delta\mathbf{x}$ will have the same frequency components as $\mathbf{x}_0$ and the new fundamental frequency will then be due to $p(t)$. If $\mathbf{x}_0$ is periodic of fundamental frequency ω_{in}, the incremental term $\Delta\mathbf{x}$ will have frequency components given by $k\omega_{\text{in}} + \omega_a$. The incremental vector $\Delta\mathbf{x}$ must satisfy the HB perturbation system, obtained when the nonlinear equations are linearized about $\mathbf{x}_0$ [4], and the resulting homogeneous system will also satisfy (9). This provides the Hopf bifurcation condition. This will be true as long as the probe amplitude remains small enough for the Taylor expansion (A.4) to be valid, which of course, implies $\mu \simeq \mu_H$.

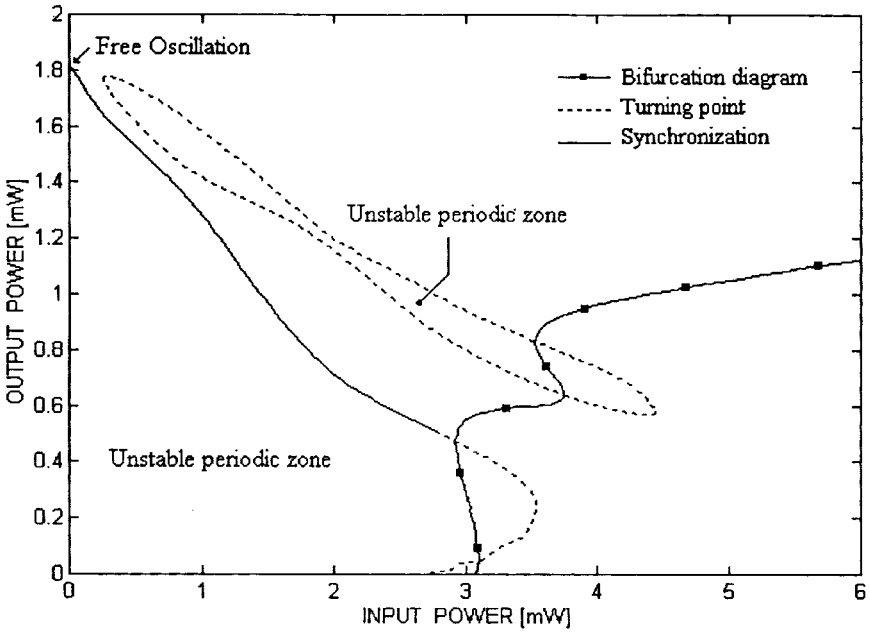

Fig. 11. Bifurcation loci on the plane input power–output power for $\omega_{\rm in} \leq 2\omega_0$. The bifurcation diagram as a function of input power for $F_{\rm in} = 26.5$ GHz has been superimposed.

B. I-Type Bifurcations

In case of an I-type bifurcation, the probe nonperturbation equations will provide a solution

$$\mathbf{S}(\overline{\mu},\, \phi_p) = 0 \quad \text{with } A_p = \epsilon \text{ and } \omega_p = \frac{\omega_{\rm in}}{2}. \tag{A.5}$$

And in this case, the probe value will be

$$p(t) = \epsilon \cos\left(\frac{\omega_{\rm in}}{2}\, t + \phi_p\right). \tag{A.6}$$

Due to the small probe value, it will be possible to carry out a Taylor expansion of $\mathbf{x}(t)$ about $p = 0$, in a similar way to (A.4). The new fundamental frequency will be now the input generator frequency divided by two. Since $\mathbf{x}$ is an HB solution, the corresponding incremental vector must satisfy the HB perturbation equations and the I-type bifurcation condition [derived from (9)] is directly obtained.

ACKNOWLEDGMENT

The authors are very grateful to M. Camiade of THOMSON-TCS, Orsay, France, for providing the MMIC divider.

REFERENCES

[1] V. Rizzoli, A. Neri, P. Ghigi, and F. Mastri, "Simulation and design of nonlinear microwave circuits: An overview of frequency domain techniques for the treatment of oscillators," in *Proc. Int. Workshop West German IEEE Chapter*, Duisburg, Germany, Oct. 1990, pp. 123–136.

[2] R. Quéré, E. Ngoya, M. Camiade, A. Suárez, M. Hessane, and J. Obregon, "Large signal design of broadband monolithic microwave frequency dividers and phase-locked oscillators," *IEEE Trans. Microwave Theory Tech.*, vol. 41, pp. 1928–1938, Nov. 1993.

[3] D. Hente and R. H. Jansen, "Frequency-domain continuation method for the analysis and stability investigation of nonlinear microwave circuits," *Proc. Inst. Elect. Eng.*, vol. 133, pt. H, no. 5, pp. 351–362, Oct. 1986.

[4] V. Rizzoli and A. Neri, "State of the art and present trends in nonlinear microwave CAD techniques," *IEEE Trans. Microwave Theory Tech.*, vol. 36, pp. 343–356, Feb. 1988.

[5] J. M. T. Thompson and H. B. Stewart, *Nonlinear Dynamics and Chaos.* New York: Wiley, 1986.

[6] J. Guckenheimer and P. Holmes, *Nonlinear Oscillations, Dynamical Systems and Bifurcations of Vector Fields.* Berlin, Germany: Springer-Verlag, 1990.

[7] C. Camacho-Peñalosa, "Numerical steady-state analysis of nonlinear microwave circuits with periodic excitation," *IEEE Trans. Microwave Theory Tech.*, vol. MTT-31, pp. 724–730, Sept. 1983.

[8] K. Kurokawa, "Some basic characteristics of broadband negative resistance oscillators," *Bell Syst. Tech. J.*, pp. 1937–1955, July/Aug. 1969.

[9] H. Kawakami, "Bifurcation of periodic responses in forced dynamic nonlinear circuits: Computation of bifurcation values of the system parameters," *IEEE Trans. Circuits Syst.*, vol. CAS-31, pp. 248–260, Mar. 1984.

[10] A. Suárez, J. C. Sarkissian, R. Sommet, E. Ngoya, and R. Quéré, "Stability analysis of analog frequency dividers in the quasi-periodic regime," *IEEE Trans. Microwave Guided Wave Lett.*, vol. 4, pp. 138–140, May 1994.

[11] J. Morales, A. Suárez, E. Artal, and R. Quéré, "Global stability analysis of self-oscillating mixers," in *Proc. 25th European Microwave Conf.*, Bologna, Italy, Sept. 1995, pp. 1216–1219.

[12] J. Morales, A. Suárez, and R. Quéré, "Accurate determination of frequency dividers operating bands," *IEEE Microwave Guided Wave Lett.*, vol. 6, pp. 46–48, Jan. 1996.

[13] A. Suárez, E. Ngoya, P. Savary, M. Camiade, J. C. Sarkissian, and R. Quéré, "Broadband design and simulation of frequency dividers in the millimetric band," in *Proc. 23rd European Microwave Conf.*, Madrid, Spain, Sept. 1993, pp. 777–780.

Almudena Suárez (M'86) was born in Santander, Spain, in 1964. She received the electronic physics and the Ph.D. degrees from the University of Cantabria, Santander, Spain, in 1987 and 1992, respectively, and the Ph.D. degree in electronics from the University of Limoges, Limoges, France, in 1993.

In 1987, she joined the Electronics Department, University of Cantabria, working on nonlinear simulation. From May 1990 to December 1992, she was on leave at the Laboratory IRCOM, University of Limoges, Limoges, France. Since 1995, she has been an Associate Professor in the Communications Engineering Department, University of Cantabria. Her areas of interest include the nonlinear design of microwave circuits and especially the nonlinear stability analysis and investigation of chaotic regimes.

Jose Morales (S'81–M'83) was born in Tachira, Venezuela, in 1963. He received the degree in electrical engineering from the University of Los Andes, Los Andes, Mérida, Venezuela, in 1987, and the Ph.D. degree from the University of Cantabria, Santander, Spain, in 1996..

From 1993 to 1997, he was on leave at the University of Cantabria, working on the development of simulation tools for the stability analysis of nonlinear microwave circuits. In October 1997, he joined the Electronic Department, University of Tachira, Tachira, Venezuela.

Raymond Quéré (M'88) received the engineer degree and the French "agrégation" degree in applical physics from E-NSEEIHT Toulouse, Toulouse, France, in 1976 and 1978, respectively, and the Ph.D. degree from the University of Limoges, Limoges, France, in 1992.

In 1989, he was appointed Professor at the Technology Institute Electrical Engineering (IUT), Brive, France. He is involved in research dealing with nonlinear design and modeling of microwave circuits with a special emphasis on nonlinear stability analysis of potentially unstable circuits such as oscillators, frequency dividers, and power amplifiers. He is also strongly involved with nonlinear characterization and modeling of microwave active devices based on pulsed measurements techniques.

Dr. Quéré is a member of the Technical Committee of the EuMC and has served as a reviewer for several issues of the IEEE TRANSACTIONS ON MICROWAVE THEORY AND TECHNOLOGY.